Competing Instabilities and Metastable States in $(Nd, Sm)_{1/2}Sr_{1/2}MnO_3$

Y. Tokura,[1,2] H. Kuwahara,[1] Y. Moritomo,[1] Y. Tomioka,[1] and A. Asamitsu[1]
[1]*Joint Research Center for Atom Technology (JRCAT), Tsukuba 305, Japan*
[2]*Department of Applied Physics, University of Tokyo, Tokyo 113, Japan*
(Received 10 October 1995)

Competition between the ferromagnetic double-exchange interaction and the antiferromagnetic charge-ordering instability gives rise to thermally as well as magnetic field (H) induced insulator-metal transitions in distorted perovskites $(Nd_{1-y}Sm_y)_{1/2}Sr_{1/2}MnO_3$ with a controlled one-electron bandwidth. A systematic study on the metal-insulator phase diagram in the T-H plane with varying y as well as a high-pressure study has revealed the metastable nature of the undercooled ferromagnetic metallic state.

PACS numbers: 71.30.+h, 71.27.+a, 71.28.+d, 75.30.Kz

Due to the versatile phenomena of colossal magnetoresistance [1] and magnetic field induced structural changes [2–4], there is increasing interest in the barely metallic ferromagnetic state of hole-doped manganese oxides with perovskite structure $RE_{1-x}AE_xMnO_3$ where RE and AE are trivalent rare earth and divalent alkaline earth ions, respectively. The ferromagnetic interaction in those compounds is mediated by the so-called double-exchange mechanism [5–8]: Itinerant doped holes can align the local spins of the $3d$ t_{2g} state ferromagnetically via a strong on-site exchange interaction (Hund coupling). In the real manganese oxide systems, however, there are many other instabilities which are competitive with the double-exchange interaction, such as the antiferromagnetic superexchange, Jahn-Teller, orbital-ordering, and charge-ordering interactions. Among them, the charge-ordering transition, i.e., the real space ordering of the doped holes, shows up in many of the hole-doped manganese oxides [3,4,9–15] as in other (layered) perovskite-type transition metal oxides [16,17], which occasionally accompany the spin and orbital ordering (and perhaps Jahn-Teller distortion) as well. In this Letter, we report on novel metal-insulator phase diagrams in the temperature–magnetic field plane and their systematics with the one-electron bandwidth of the e_g state as a consequence of competition between the double-exchange and charge-ordering interactions. (In our nomenclature, the term "charge ordering" stands for the accompanying lattice distortion as well.)

The system investigated here is $(Nd_{1-y}Sm_y)_{1/2}Sr_{1/2}MnO_3$ with an orthorhombically distorted perovskite structure (of the $GdFeO_3$ type), where the nominal hole concentration x is fixed at $1/2$, i.e., one e_g-state hole (or electron) per two Mn sites, and, hence, the charge-ordered state tends to be most stabilized [10,12]. We have systematically controlled the hopping interaction of the e_g electron or its one-electron bandwidth (W) with varying ionic radius of the perovskite A site [the (Nd, Sm, Sr) site in the present case]. Depending on the averaged ionic radius of the perovskite A site, the bond angle (θ) of Mn-O-Mn shows a deviation from 180° in the orthorhombic lattice. The smaller the ionic radius of the A site is, the narrower W is [18,19]. This is because W for the hole-doped manganese oxides is governed by the degree of the hybridization between the Mn $3d$ e_g state and O $2p$ σ state which approximately scales as $\cos^2\theta$. The double-exchange interaction arises from the itineracy of the doped holes, and, hence, the reduction in W destabilizes the ferromagnetic state [19]. The competition between the ferromagnetic and charge-ordered states is so sensitive to W that we need to control W to reveal the whole systematics. For this purpose, we have prepared a series of crystals with finely controlled ionic radii of the A sites, $(Nd_{1-y}Sm_y)_{1/2}Sr_{1/2}MnO_3$, in which the relative change of the W value is expected to be (5–7)% judging from a difference of the Mn-O-Mn bond angle ($\Delta\theta \approx 3°$) in the $A = Nd_{1/2}Sr_{1/2}$ ($y = 0$) and $A = Sm_{1/2}Sr_{1/2}$ ($y = 1$) crystals [20]. The crystals were grown by the floating zone method with the use of a lamp-image furnace [21]. The electron-probe microanalysis, as well as the inductively coupled plasma mass spectroscopy (ICP) on the respective crystals, indicated that the stoichiometry is accurately in accord with the prescribed one within a relative error of ± 0.01.

We show in Fig. 1 the temperature dependence of the resistivity in $(Nd_{1-y}Sm_y)_{1/2}Sr_{1/2}MnO_3$ crystals ($y = 0$, 0.5, 0.75, and 0.875) under various external magnetic fields. (The current direction with respect to the crystallographic axis was not specified.) In the $Nd_{1/2}Sr_{1/2}MnO_3$ ($y = 0$) crystal, the resistivity shows a decrease at about 255 K which corresponds to the onset of the ferromagnetic state. With further decrease of temperature, the resistivity shows an abrupt jump at 150 K. This resistivity anomaly corresponds to the phase change from the ferromagnetic metal to antiferromagnetic insulator due to the onset of the charge-ordered (CO) state in which the Mn sites are occupied by the nominal Mn^{3+} and Mn^{4+} species with 1:1 ratio [3,4]. A recent neutron scattering study [22] has confirmed that the charge- and spin-ordering pattern is the same as in $La_{1/2}Ca_{1/2}MnO_3$ [23] and $Pr_{1/2}Ca_{1/2}MnO$ [9]: There is alternating charge density on the (001) plane and the unit cell for the ordered spins is $4 \times 4 \times 2$ (of the CO type) in the pseudocubic setting of the perovskite.

Application of an external magnetic field for the $y = 0$ crystal reduces the resistivity around the Curie

 0031-9007/96/76(17)/3184(4)$10.00

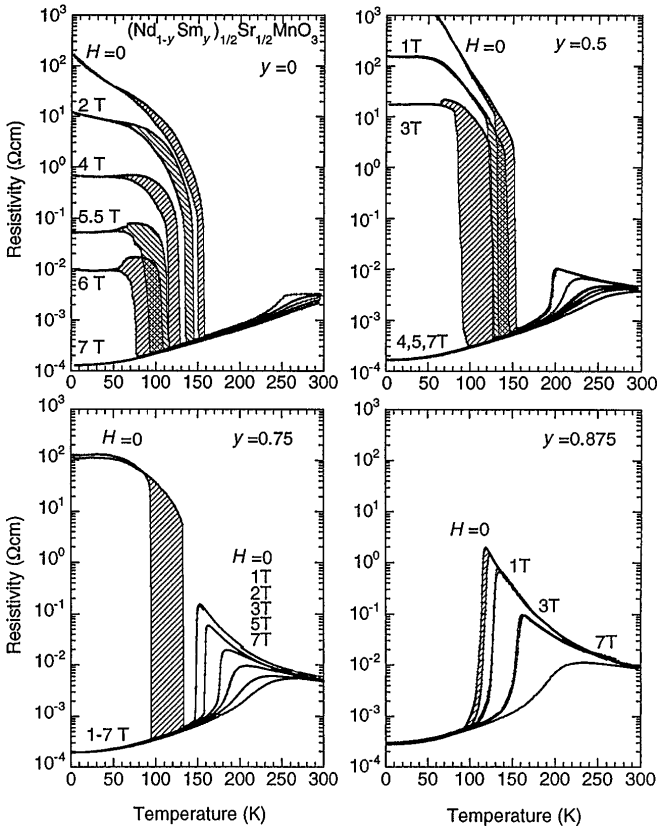

FIG. 1. Temperature dependence of resistivity under various magnetic fields for $(Nd_{1-y}Sm_y)_{1/2}Sr_{1/2}MnO_3$ with $y = 0$, 0.5, 0.75, and 0.875. A pair of curves allotted to each magnetic field correspond to the cooling and warming runs, and the hatched area represents a thermal hysteresis.

temperature T_C (= 255 K) due to the reduced spin scattering by the field induced alignment of the local spins, which is similar to the case of $La_{1-x}Sr_xMnO_3$ [21]. A more remarkable field effect is that the charge-ordering phase transition (associated with a change in the lattice parameters [24]) is suppressed while the ferromagnetic metallic (FM) region is extended to lower temperature. Under a field above 7 T, the charge-ordered antiferromagnetic insulating state (AFI) is totally extinguished down to zero temperature. Apart from a difference in the hysteretic behavior, the observed behavior for $Nd_{1/2}Sr_{1/2}MnO_3$ ($y = 0$) resembles that for $Pr_{1/2}Sr_{1/2}MnO_3$ [3] which has recently been known to show a similar charge-ordering phase transition.

A change in the A-site composition y in $(Nd_{1-y}Sm_y)_{1/2}Sr_{1/2}MnO_3$ causes a remarkable variation in the temperature dependence of the resistivity and magnetoresistance as seen in Fig. 1. The resistivity drop at 197 K ($y = 0.5$), 148 K ($y = 0.75$), and 115 K ($y = 0.875$) corresponds to the transition to the FM state. The resistivity immediately above T_C remarkably increases with y (perhaps due to the enhanced electron-lattice coupling, e.g., dynamic and collective Jahn-Teller coupling [25]), and the resistivity drop is hence remarkably enhanced, while T_C decreases with y. As a result, the charge-ordering transition temperature (T_{CO}), at which the compound undergoes the FM to AFI transition showing a resistivity jump, appears to approach T_C with increasing y up to $y = 0.75$. The observed continuous decrease of T_C with y can be understood in terms of a decrease of the one-electron bandwidth W [19]: The increased Mn-O-Mn bond distortion with y reduces W, as described above, which weakens the ferromagnetic double-exchange interaction but may relatively enhance the charge-ordering instability. For the $y = 0.875$ crystal, however, the FM state below $T_C = 115$ K appears to persist down to zero temperature and there is no trace of the FM-to-AFI transition at lower temperatures. Such a sudden disappearance of the low-temperature CO state between $y = 0.75$ and 0.875 is, therefore, apparently against the simply expected behavior. We have to consider the metastable nature of the FM state as discussed in the following.

The magnetic field effect on the FM-to-AFI transition (i.e., the charge-ordering phase transition) is even more critically dependent on the lattice form than the transition temperature itself. The low-temperature AFI phase with larger y is more amenable to an external field which tends to stabilize the FM phase. For example, the AFI state disappears at a field above 4 T for $y = 0.5$ and above 1 T for $y = 0.75$ and is absent even at zero field for $y = 0.875$, as seen in the resistivity curves shown in Fig. 1. Thus, the systematics with y seem to hold good as far as we consider the M-I (metal-insulator) phase diagram in the temperature–magnetic field plane.

We exemplify in Fig. 2 the change of the resistivity with an external magnetic field (isothermal magnetoresistance) at several temperatures for the $y = 0.75$ crystal. Corresponding to the collapse of the CO state, the field induced I-M transition takes place accompanying a change of the resistivity by several orders of magnitude. Upon this transition, the magnetization was observed to show a metamagnetic transition, and, hence, the transition can be viewed as a field induced AFI-FM transition [3]. The respective magnetoresistance curves show critically temperature-dependent hystereses. The two curves at 115 K (within the thermal hysteresis region at zero field) in Fig. 2 corresponds to the runs starting from the FM state and the AFI (once cooled below 90 K and then warmed) state, respectively. The I-M transition becomes irreversible near T_C (e.g., at 115 K) and also at lower temperatures below 40 K (e.g., at 10 K).

On the basis of such isothermal magnetoresistance data for a series of crystals, $(Nd_{1-y}Sm_y)_{1/2}Sr_{1/2}MnO_3$, we determined the M-I phase diagrams in the T-H planes (Fig. 3) for the $y = 0$, 0.5, 0.75, and 0.875 crystals. (The M-I phase diagram is least affected by the direction of H.) Open and closed circles in Fig. 3 represent the critical fields for the AFI-to-FM and FM-to-AFI transitions, respectively. With a decrease in temperature, the hysteretic field region is remarkably expanded as typically seen in the diagram for $y = 0$. This is perhaps a generic feature for the first-order phase transition occurring at low

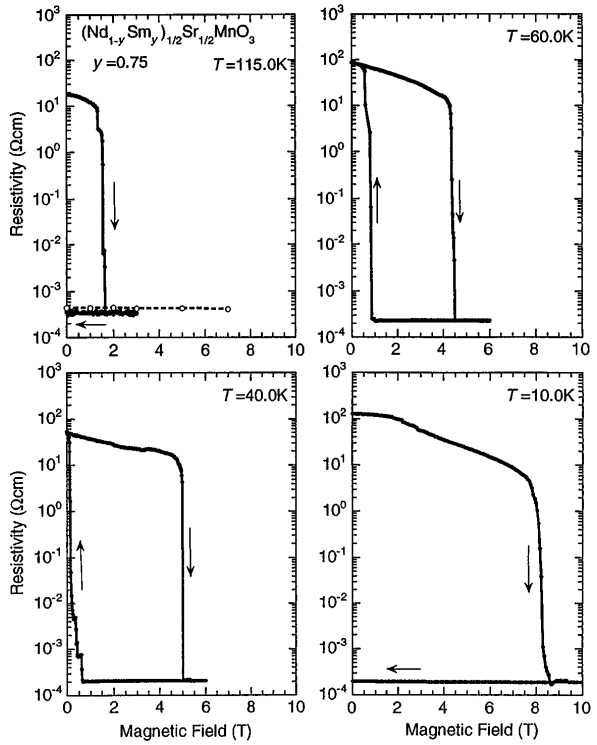

FIG. 2. Isothermal magnetoresistance and its hysteretic behavior for $(Nd_{1-y}Sm_y)_{1/2}Sr_{1/2}MnO_3$ ($y = 0.75$) crystal. The two curves at 115 K within the thermal hysteresis correspond to the runs starting from the metallic state (a dotted line) and the insulating state (once cooled below 90 K and then warmed; a solid line).

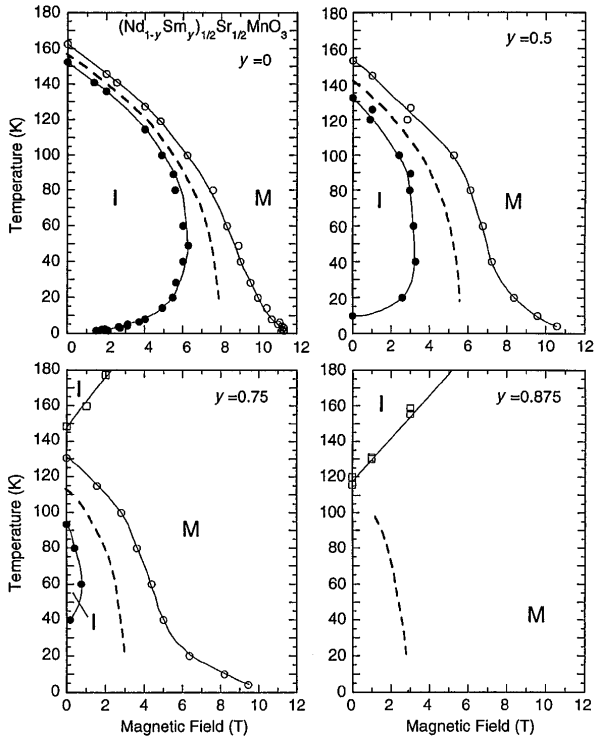

FIG. 3. The metal-insulator phase diagrams in the temperature–magnetic field plane for $(Nd_{1-y}Sm_y)_{1/2}Sr_{1/2}MnO_3$ with $y = 0$, 0.5, 0.75, and 0.875. Open and closed circles represent the critical magnetic fields for the transitions from charge-ordered antiferromagnetic insulator to ferromagnetic metal and *vice versa*, respectively. Open squares for the $y = 0.75$ and 0.875 crystals represent the first-order phase change to the ferromagnetic metallic state accompanying a change in lattice parameters. Dashed lines are the postulated boundary for the thermodynamically stable states (see text).

temperatures: When the potential barrier between the FM and AFI states is high enough compared to thermal energy, the transition probability of the metastable state (either FM or AFI) is reduced as a result of suppression of thermal fluctuation, producing a sort of undercooled state as observed [4]. The dashed lines in the phase diagrams of Fig. 3 represent the postulated true phase boundaries for the thermodynamically stable state, which was tentatively taken as the midpoint $[H_c = (H_i + H_d)/2]$ of the lower (H_d) and upper (H_i) critical fields at a fixed temperature.

The M-I phase diagrams in the T-H plane shows a characteristic variation with y, as shown in Fig. 3. With an increase in y, the M-I phase boundary shifts toward a lower field as a whole, and hysteretic behavior becomes even more prominent: The lower critical field H_d for the M-to-I transition (indicated by closed circles) decreases and becomes zero at some finite temperature; e.g., at 10 K for $y = 0.5$ and at 40 K for $y = 0.75$. Below these temperatures, the field induced I-M transition becomes irreversible, accompanying an almost permanent (on a laboratory time scale) change of the resistivity by several orders of magnitude. With an increase in y, the insulator phase region is restricted to a lower field region and narrower temperature region, and finally disappears in the T-H plane, e.g., for $y = 0.875$. It is worth noting that below this critical y value the upper critical field (indicated by open circles in Fig. 3) for the AFI-FM transition also disappears since only the FM state shows up in the low-temperature region, as observed for $y = 0.875$ in Fig. 1. However, this does not necessarily mean that the FM state is thermodynamically stable below T_C. We have roughly estimated the averaged critical field H_c as a true phase boundary (indicated by dashed lines in Fig. 3) for the $y = 0.875$ crystal by extrapolating the H_c values at lower y values at each temperature. According to the phase diagram for $y = 0.875$ (Fig. 3), the FM state at zero field is mostly (at least below 100 K) metastable in nature. In other words, the FM state below about 100 K persists down to zero temperature as an undercooled state.

The appearance of the metastable state seems to be generic for the phase transition with two competing order parameters, that is, the ferromagnetic magnetization and the charge ordering in the present case. In fact, it has been shown in terms of Landau theory [26] that the biquadratically coupled (and strongly competing) order parameters can give rise to a first-order transition line when one order parameter (say, the magnetization in the present case) orders first at higher temperature, but the free energy is lower for the ordering of the other parameter (say, the charge ordering) at lower temperature. Such an

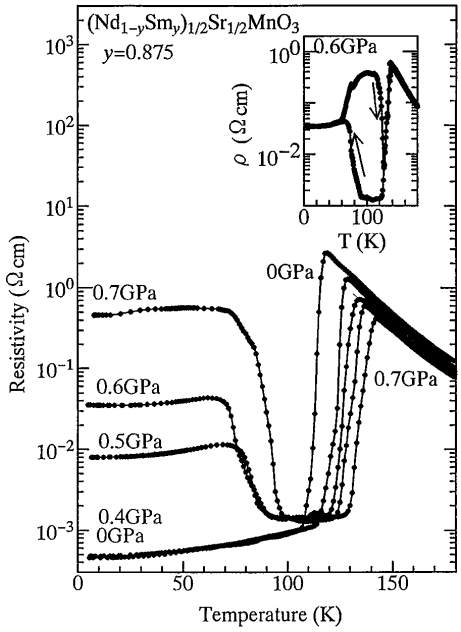

FIG. 4. Temperature dependence (in the cooling run) of resistivity under quasihydrostatic pressures for $(Nd_{1-y}Sm_y)_{1/2}Sr_{1/2}MnO_3$ ($y = 0.875$). The inset exemplifies thermally hysteretic behavior under pressure.

undercooled nature of the low-temperature ferromagnetic phase shows up also in the "inverse" pressure effect on the *M-I* transition in the present system. We have measured the resistivity under quasihydrostatic pressures for the $x = 0.875$ crystal with use of a piston cylinder type pressure cell. The results of the cooling runs are shown in Fig. 4. (A thermal hysteresis is observed, as exemplified in the inset of Fig. 4, similarly to the case shown in Fig. 1.) The T_C for the FM transition, which shows up as a distinct edge of the resistivity curve in Fig. 4, steadily increases with pressure, 115 K at 0 GPa to 145 K at 0.7 GPa, indicating that the pressure increases *W* as expected. On the other hand, application of pressure induces the *M*-to-*I* transition at low temperature; namely, the low-temperature CO state is revived by pressure. We should notice again here that the FM state in the present case is metastable in nature and that pressure appears to induce the decay of this metastable state into the thermodynamically stable state (namely, AFI). Thus the metastable state and its transitions sensitive to temperature, magnetic field, and pressure are the key to novel *M-I* phenomena (or so-called colossal magnetoresistance effects) in the present system and perhaps also in many other perovskites of manganese oxide with such competing double-exchange and charge-ordering interactions.

The present work was supported by the New Energy and Technology Development Organization (NEDO) of Japan and by a Grant-in-Aid for Scientific Research from the Ministry of Education, Science and Culture, Japan.

[1] For examples at an early stage of the research, see R. M. Kusters, S. Singleton, D. A. Keen, R. McGreevy, and W. Heyes, Physica (Amsterdam) **155B**, 362 (1989); S. Jin, T. H. Tiefel, M. McCormack, R. A. Fastnacht, R. Ramesh, and L. H. Chen, Science **264**, 413 (1994).
[2] A. Asamitsu, Y. Moritomo, Y. Tomioka, T. Arima, and Y. Tokura, Nature (London) **373**, 407 (1995).
[3] Y. Tomioka, A. Asamitsu, Y. Moritomo, H. Kuwahara, and Y. Tokura, Phys. Rev. Lett. **74**, 5108 (1995).
[4] H. Kuwahara, Y. Tomioka, A. Asamitsu, Y. Moritomo, and Y. Tokura, Science (to be published).
[5] C. Zener, Phys. Rev. **82**, 403 (1951).
[6] P. W. Anderson and H. Hasegawa, Phys. Rev. **100**, 675 (1955).
[7] P.-G. de Gennes, Phys. Rev. **118**, 141 (1960).
[8] K. Kubo and N. Ohata, J. Phys. Soc. Jpn. **33**, 21 (1972).
[9] Z. Jirak, S. Krupicka, V. Nekvasil, E. Pollert, G. Villeneuve, and F. Zounova, J. Magn. Magn. Mater. **15–18**, 519 (1980); Z. Jirak, S. Krupicka, Z. Simsa, M. Dlouha, and Z. Vratislav, J. Magn. Magn. Mater. **53**, 153 (1985).
[10] K. Knizek, Z. Jirak, E. Pollert, F. Zounova, and S. Vratislav, J. Solid State Chem. **100**, 292 (1992).
[11] Y. Tomioka, A. Asamitsu, Y. Moritomo, and Y. Tokura, J. Phys. Soc. Jpn. **64**, 3626 (1995).
[12] Y. Tomioka, A. Asamitsu, H. Kuwahara, Y. Moritomo, and Y. Tokura, Phys. Rev. B **53**, R1689 (1996).
[13] H. Yoshizawa, H. Kawano, Y. Tomioka, and Y. Tokura, Phys. Rev. B **52**, R13 145 (1995).
[14] Y. Moritomo, Y. Tomioka, A. Asamitsu, and Y. Tokura, Phys. Rev. B **51**, 3297 (1995).
[15] P. Schiffer, A. P. Ramirez, W. Bao, and S-W. Cheong, Phys. Rev. Lett. **75**, 3336 (1995).
[16] P. D. Battle, T. C. Gibb, and P. Lightfoot, J. Solid State Chem. **84**, 271 (1990).
[17] C. H. Chen, S-W. Cheong, and A. S. Cooper, Phys. Rev. Lett. **71**, 2461 (1993).
[18] J. B. Torrance, P. Laccore, A. I. Nazzal, E. J. Ansaldo, and Ch. Niedermayer, Phys. Rev. B **45**, 8209 (1992).
[19] H. Y. Hwang, S-W. Cheong, P. G. Radaelli, M. Marezio, and B. Batlogg, Phys. Rev. Lett. **75**, 914 (1995).
[20] An empirical relation between the *A*-site ionic radius and the metal-oxygen-metal bond angle was derived for the orthorhombically distorted ($GdFeO_3$-type) perovskite oxides; M. Marezio, J. P. Remeika, and P. D. Dernier, Acta Crystallogr., Sect. B **26**, 2008 (1970); D. A. MacLean, H-N. Ng, and J. E. Greedan, J. Solid State Chem. **30**, 35 (1979).
[21] Y. Tokura, A. Urushibara, Y. Moritomo, T. Arima, A. Asamitsu, G. Kido, and N. Furukawa, J. Phys. Soc. Jpn. **63**, 3931 (1994); A. Urushibara, Y. Moritomo, T. Arima, A. Asamitsu, G. Kido, and Y. Tokura, Phys. Rev. B **51**, 14 103 (1995).
[22] H. Yoshizawa, H. Kawano, H. Kuwahara, and Y. Tokura (unpublished).
[23] E. O. Wollan and W. C. Koehler, Phys. Rev. **100**, 545 (1955).
[24] The orthorhombic lattice parameters ($a \approx b \approx \sqrt{2}\,a_p$ and $c \approx 2a_p$, with a_p for a cubic perovskite) show an abrupt change [4] upon the CO transition: The lattice constants *a* and *b* expand by ≈0.5% while *c* shrinks by ≈1.2%.
[25] A. J. Millis, P. B. Littlewood, and B. I. Shraiman, Phys. Rev. Lett. **74**, 5144 (1995); A. J. Millis, B. I. Shraiman, and R. Mueller (to be published).
[26] For example, Y. Imry, J. Phys. C **8**, 567 (1975).